Diurnal variations of temperature and winds inferred from TIMED and UARS measurements

Frank T. Huang,[1] Hans G. Mayr,[2] Carl A. Reber,[2] Timothy Killeen,[3] James Russell,[4] Marty Mlynczak,[5] Wilbert Skinner,[6] and John Mengel[7]

Received 13 September 2005; revised 17 March 2006; accepted 11 April 2006; published 15 September 2006.

[1] Owing to their sampling properties in local solar time, both the TIMED and UARS spacecrafts provide the opportunity to quantitatively study the mesospheric thermal tides. The information though is limited because it takes the TIMED instruments 2 months to cover the full range of 24 hours, almost twice as long as UARS. We present here the results of an analysis, in which the seasonal and global-scale variations of amplitude and phase for the migrating diurnal tide are retrieved from atmospheric temperature and wind measurements on the TIMED (SABER, TIDI) and UARS (MLS, HRDI) satellites. Comparisons are made with results from the Numerical Spectral Model (NSM), which is characterized in part by the parameterization of small-scale gravity waves. At 60 km and above, the amplitude and phase variations of the diurnal tide from the NSM agree generally well with those derived from the SABER temperatures. In the SABER temperature amplitudes at around 60 km there are evident asymmetries in latitude with respect to the equator, which are not apparent in the MLS data near 55 km or in the NSM. (The asymmetry in the SABER temperatures disappears above 60 km.) For the meridional winds of the migrating diurnal tide derived from TIDI, the phase and relative amplitude variation with latitude and season are in qualitative agreement with the HRDI measurements and the NSM. The amplitudes from TIDI winds are systematically smaller, but this may in part be due to interannual variations. However, the results for the zonal winds from TIDI more often do not agree well with those from HRDI or the NSM.

Citation: Huang, F. T., H. G. Mayr, C. A. Reber, T. Killeen, J. Russell, M. Mlynczak, W. Skinner, and J. Mengel (2006), Diurnal variations of temperature and winds inferred from TIMED and UARS measurements, *J. Geophys. Res.*, *111*, A10S04, doi:10.1029/2005JA011426.

1. Introduction

[2] In recent decades, our understanding of the atmosphere dynamics and energetics has advanced considerably. However, there had been a dearth of global, long-term wind and temperature observations for the middle atmosphere and thermosphere until measurements became available from the Thermosphere-Ionosphere-Mesosphere-Energetics and Dynamics (TIMED) satellite and the Upper Atmosphere Research Satellite (UARS) [*Reber*, 1993]. The temperature measurements are made on TIMED by the Sounding of the Atmosphere using Broadband Emission Radiometry (SABER) [*Russell et al.*, 1999] and on UARS by the Microwave Limb Sounder (MLS) [*Barath et al.*, 1993]. The wind observations are carried out on TIMED by the Doppler Interferometer (TIDI) [*Killeen et al.*, 1999] and on UARS by the High Resolution Doppler Imager (HRDI) [*Hays et al.*, 1993].

[3] Previous results of migrating tides based on wind measurements from HRDI on UARS include those by *Burrage et al.* [1995, 1996], and *Huang and Reber* [2003], while *McLandress et al.* [1996] derived migrating tide results of winds based on data from the Wind Imaging Interferometer (WINDII, also on UARS). Major results from these analyses included variations of tides over a wide latitude, altitude, and time ranges, which were not previously available. Examples are the variations of tidal amplitudes and phases over a period of 1 year and longer, including the dominant semiannual variation in the amplitude of the diurnal tide, and their variations with latitude. *Forbes et al.* [2003], *Manson et al.* [2002], and *Huang and Reber* [2004] derived corresponding nonmigrating tides based on HRDI wind measurements.

[4] TIMED and UARS were launched about 10 years apart (December 2001 and September 1991, respectively), providing data to study variations over a decade or more. The measurements on TIMED concentrate mainly on the mesosphere and thermosphere while those on UARS focus

[1]Creative Computing Solutions Inc., Rockville, Maryland, USA.
[2]NASA Goddard Space Flight Center, Greenbelt, Maryland, USA.
[3]High Altitude Observatory, National Center for Atmospheric Research, Boulder, Colorado, USA.
[4]Center for Atmospheric Sciences, Hampton University, Hampton, Virginia, USA.
[5]NASA Langley Research Center, Hampton, Virginia, USA.
[6]Department of Atmospheric, Oceanic, and Space Sciences, University of Michigan, Ann Arbor, Michigan, USA.
[7]Science Systems and Applications, Lanham, Maryland, USA.

0148-0227/06/2005JA011426

on the middle atmosphere, but there are regions of overlap. For example, SABER measures temperatures from the tropopause into the thermosphere, and HRDI measured winds from the stratosphere into the mesosphere. TIMED and UARS also have common sampling properties in local solar time, and this provides the opportunity to quantitatively study the winds and temperatures of the diurnal tides, which are the dominant dynamical features of the mesosphere. We present here the results from an analysis of SABER and MLS temperatures and TIDI and HRDI winds to describe the seasonal and latitudinal variations of the migrating diurnal tides.

[5] Much of our understanding of the middle atmosphere can be attributed to theoretical studies going back several decades, and we refer to the classical text on atmospheric tides by *Chapman and Lindzen* [1970]. *Lindzen* [1981] proposed that gravity wave drag can produce the observed temperature anomaly in the upper mesosphere (colder in summer than in winter), and in several subsequent studies the mechanism was confirmed [e.g., *Holton*, 1982; *Gaertner et al.*, 1983; *Geller*, 1984; *Garcia and Solomon*, 1985]. Gravity wave (GW) interactions have also been invoked to study the migrating and nonmigrating diurnal tides [e.g., *McLandress*, 1997, 2002a, 2002b; *Norton and Thuburn*, 1999; *Meyer*, 1999; *Hagan et al.*, 1999; *Akmaev*, 2001a, 2001b; *Mayr et al.*, 1998, 2001, 2005a, 2005b]. In the upper mesosphere, the amplitude of the diurnal tide exhibits pronounced maxima near equinox, which have been attributed to variations in eddy viscosity [e.g., *Geller et al.*, 1997; *Yudin et al.*, 1997; *Akmaev*, 2001b] and to the seasonal variations of the meridional advection associated with the zonal circulation [*McLandress*, 2002b]. Momentum deposition from GWs was shown to amplify the equinoctial maxima of the diurnal tide [*Mayr et al.*, 1998, 2001]. However, when the GW drag is applied in a form similar to Rayleigh friction, as in some models, the effect dampens the tides. The results of *Norton and Thuburn* [1999] suggest that GW interactions are not necessary, and probably not important, for the semiannual variation of the diurnal tide.

[6] In section 2, we describe the temperature and wind measurements from TIMED and UARS. In section 3 we discuss the sampling properties of the two spacecrafts and describe the algorithm that is applied in the analysis of the data. We compare the observations with recent numerical results [*Mayr et al.*, 2005a, 2005b] obtained from the Numerical Spectral Model (NSM). The NSM incorporates Hines' Doppler Spread Parameterization for GWs, and the model is briefly described in section 4. In section 5, the observations are presented for the migrating tides in comparison with the model predictions, and our conclusions are given in section 6.

2. Satellite Observations

[7] The temperature measurements on the TIMED spacecraft are from the Sounding of the Atmosphere using Broadband Emission Radiometry instrument (SABER) [*Russell et al.*, 1999], and on UARS they are obtained from the Microwave Limb Sounder (MLS) [*Barath et al.*, 1993]. The wind measurements on TIMED come from the Doppler Interferometer (TIDI) [*Killeen et al.*, 1999] and on UARS from the High Resolution Doppler Imager (HRDI) [*Hays et al.*, 1993]. The SABER instrument measures the emitted radiation at 4.3 μm and 15 μm wavelengths as it views the Earth's limb, and the kinetic temperature is retrieved by applying radiative transfer analysis. Level-2 data provided by the SABER team for the measurement footprint were interpolated to fixed altitude surfaces and latitudes. The TIDI instrument measures neutral winds from the Doppler shift of airglow (OI 557.7 nm and O_2(0-0)). The TIDI data used are the level 3 vector data files, which are provided by the TIDI team for altitudes from 70 to 105 km in increments of 2.5 km.

[8] On UARS, the measurements are restricted to the stratosphere around 55 km and below for the temperatures (MLS) and to 95 km (the only altitude at which daytime and nighttime measurements were made) for the winds (HRDI). The TIMED measurements of temperature and winds cover a larger altitude range and overlap with those from UARS. The instruments on both spacecrafts are atmospheric limb viewers, and they sample the data at different latitudes because of the north/south motion of the satellites. Different longitudes are sampled due to the rotation of the Earth relative to the orbital plane, and therefore it takes up to one day to make measurements over the globe. The satellite measurements are then not synoptic, meaning that they do not sample the data over the globe simultaneously, which is why the retrieval of tidal information is not straightforward. On the other hand, models provide results over the globe at one instant (they are synoptic, as in a snapshot). For comparison with global models, it is therefore desirable to cast the observations in a similar manner, as feasible.

[9] While the TIMED and UARS spacecrafts are not Sun-synchronous, they still sample at only two local times around a latitude circle at any given day. However, unlike Sun-synchronous satellite orbits, those of TIMED and UARS precess slowly due to the respective inclinations of 74° and 57°. For a given latitude and orbital mode (ascending or descending), the local times sampled with TIMED and UARS decrease by about 12 and 20 min, respectively, from day to day. Over a period of 60 days, using both orbital modes, TIMED thus samples the full range of local times (36 days for UARS). During the same periods, however, the measured parameters can also change due to seasonal variations and other variables. The information content in terms of local solar time is therefore somewhat limited for the measurements from UARS and even more so from TIMED. This constraint though is somewhat reduced in the case of the TIDI instrument on TIMED, which can view the atmosphere from both sides of the observatory to sample additional local times.

[10] To overcome the above-discussed limitations, our analysis uses an algorithm that estimates together the diurnal variations and their seasonal variations, as described in section 3. More details are given by *Huang and Reber* [2001, 2003]. The algorithm estimates the coefficients of a two-dimensional Fourier series at a given latitude and altitude, with the independent variables being local solar time and day-of-year. In the present paper, we describe the results for the migrating diurnal tide.

[11] In addition to the tides, the atmosphere also exhibits seasonal, interseasonal, and interannual variations in the zonal mean, prominent examples being the annual and semiannual variations and the QBO. Depending on latitude,

the amplitudes of these zonal-mean (i.e., local time and longitude independent) variations can be comparable to those of the diurnal tides. Together with the diurnal tides, we therefore estimate with our analysis also the zonal mean variations, which are presented in a separate paper.

3. Data Analysis

[12] *Huang and Reber* [2001, 2003] described in detail the algorithm that will be applied in our analysis of the TIMED and UARS observations to describe the migrating diurnal tides, and for completeness we summarize here the essential features of the analysis. For a given latitude, longitude, and altitude (pressure), the algorithm is formulated with a two-dimensional Fourier series, and a least squares analysis is performed to estimate the variations of temperatures and winds,

$$\Psi(t_l, d, z, \theta) = \sum_n \sum_m b_{nm}(z, \theta) e^{i2\pi n t_l} e^{i2\pi m d/365} \qquad (1)$$

yielding the set of coefficients $b_{nm}(z, \theta)$.

[13] Here $\Psi(t_l, d, z, \theta)$ represent the data averaged in longitude around a latitude circle, n and m are integer wave numbers, and the independent variables are local solar time and day of year, with z, altitude (or pressure surface); θ, colatitude; λ, longitude; d, day of year; t_l, local solar time (fraction of a day); and $t_l = t + \lambda/(2\pi)$, t being universal time. As is the norm, the sum in the series includes also complex conjugates (i.e., negative indices).

[14] This representation can and has been used in a more general form to describe also the nonmigrating tides with longitudinal variations [*Huang and Reber*, 2004]. The algorithm minimizes the sum of the squares of differences between the Fourier series (equation (1)) and the data covering a period of 365 days. In this least squares analysis, all the data are incorporated individually without any averaging or binning. Once the coefficients are estimated, both the zonal mean components and the variations with local solar time can be calculated directly from (1) for any day of year. For the zonal wave number, a maximum value of n = 2 is applied so that the diurnal and semidiurnal migrating tides can be estimated. Since it takes 36 days for UARS to sample the full range of local solar times, we use a maximum of m = 10 to describe the zonal mean. For the diurnal and semidiurnal coefficients, we ignore the day-of-year variations with periods less than seasonal (<3 months, or m > 4). For TIDI and SABER on TIMED, the cutoff wave number for the seasonal variations of the tides is even smaller, i.e., m = 2 or 3 (i.e., less than 4 months).

4. Numerical Spectral Model (NSM)

[15] The numerical results shown here are taken from a study with the Numerical Spectral Model (NSM), which describes the migrating and nonmigrating tides in the mesosphere under the influence of parameterized gravity waves [*Mayr et al.*, 2005a, 2005b].

[16] The NSM is fully nonlinear and time dependent, and it extends from the Earth's surface into the thermosphere at 240 km in the present application. For the zonal mean, the NSM is driven in the mesosphere and stratosphere by solar heating from UV radiation [*Strobel*, 1978] and by EUV radiation in the thermosphere. In the troposphere, a zonal-mean heat source is adopted to simulate the observed features of the zonal circulation and temperature variations around the tropopause. For the solar driven migrating tides, the heating rates in the middle atmosphere and troposphere are taken from *Forbes and Garrett* [1979]. The nonmigrating tides are produced by nonlinear interactions between migrating tides and planetary waves, but the latter are solely generated by instabilities [*Mayr et al.*, 2004] since the model does not have topography. The radiative loss is described in terms of Newtonian cooling, which is taken from the parameterization of *Zhu* [1989].

[17] An integral part of the NSM is that it incorporates the Doppler Spread Parameterization (DSP) for small-scale gravity waves (GW) formulated by *Hines* [1997a, 1997b], and its detailed application is discussed by *Mayr et al.* [2005a, 2005b]. The DSP has been extensively discussed in the literature and has been applied successfully in a number of models [e.g., *Akmaev*, 2001a, 2001b; *Manzini et al.*, 1997; *McLandress*, 2002a, 2002b]. In the DSP, a spectrum of waves interact with each other to produce Doppler spreading, which affects the interactions of the waves with the background flow. The GWs are assumed to originate in the troposphere (7.5 km), and the source is isotropic and independent of latitude and season. With adjustable parameters, the DSP provides altitude dependent eddy diffusion rates, which are assumed for simplicity to be globally uniform and time-independent. The GW generated heating rates are ignored in the model.

[18] Formulated with spherical harmonics, P_l^m, the NSM is run with a time step of about 5 min and a vertical step size of 0.5 km (below 120 km) to resolve the GW interactions with the flow. The NSM is truncated at the zonal and meridional wave numbers $m = 4$ and $l = 12$, respectively.

5. Analysis Results

5.1. Kinetic Temperatures

[19] In Figure 1, we show the derived amplitude and phase for the diurnal migrating tide temperatures at 95 km, plotted versus latitude based on SABER (asterisks) data from years 2002 and 2003. The upper row is for day 80 to represent spring, and the bottom row is for day 172 to represent northern summer. The triangles represent the results from the NSM averaged over 4 years. There is generally good agreement between the measurements and the NSM. The amplitudes from the model however are somewhat larger, and the observed phase shows more of a hemispherical asymmetry at solstice.

[20] The seasonal variations of the temperature amplitude, plotted versus latitude, are presented in Figure 2 for the diurnal migrating tide at 95 km. In the left plot are shown the derived SABER results (years 2002 and 2003 merged) and on the right are the results from the NSM (4-year average). The measurements and model result reveal the characteristic semiannual variations with maxima near equinox. However, the model does not reproduce the large difference between spring and fall equinox seen in the SABER data.

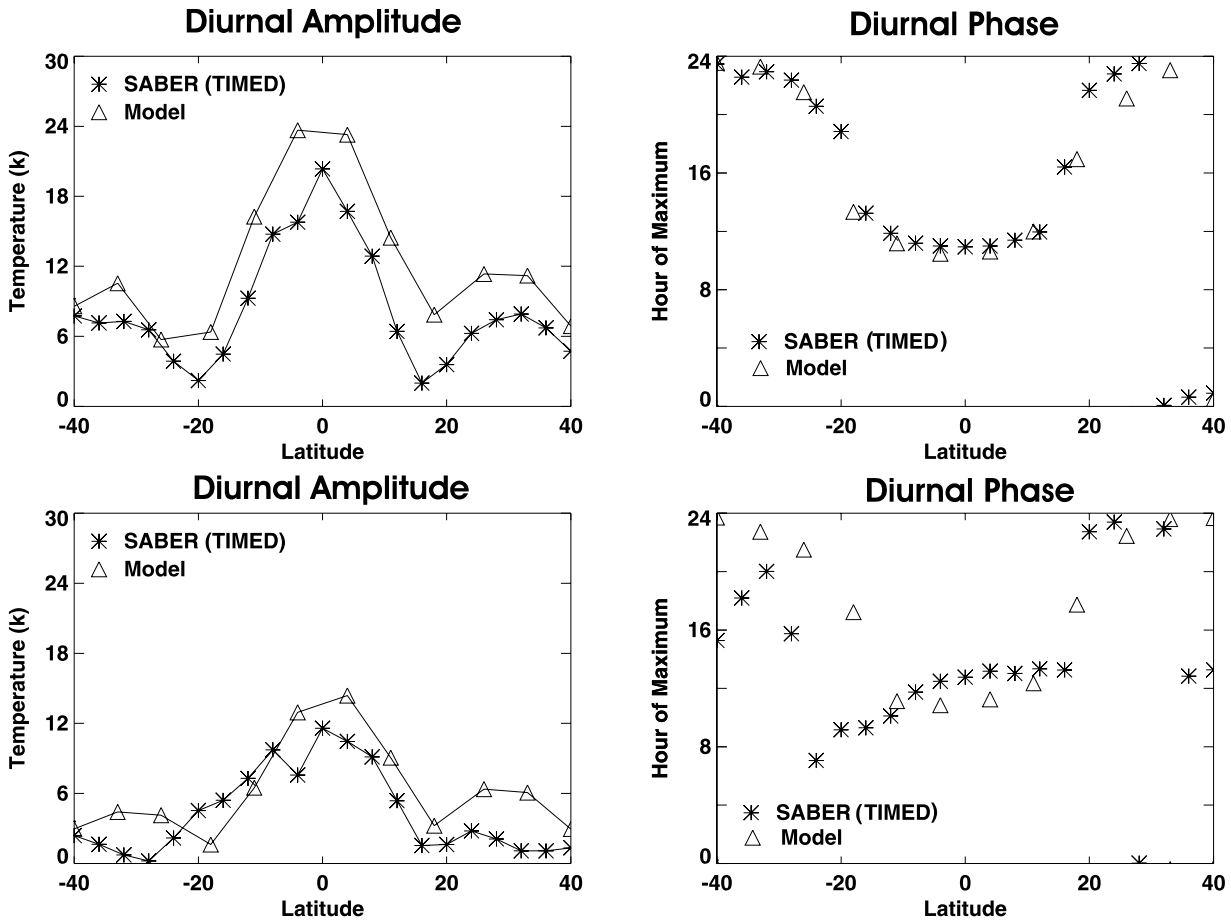

Figure 1. Amplitude and phase for the temperatures of the migrating diurnal tide at 95 km versus latitude, top for day 80 (spring) and bottom for day 172 (summer): SABER for years 2002 and 2003 compared with 4-year average from NSM.

[21] Corresponding to Figure 1, we present with Figure 3 the amplitude and phase for the temperature of the diurnal tide at 55 km, including for comparison results based on UARS measurements from the MLS instrument for the years 1992 to 1994. The upper row again applies to spring and the lower one applies to summer in the northern hemisphere. As can be seen, the variations in the SABER phase compare well with the model, but the SABER

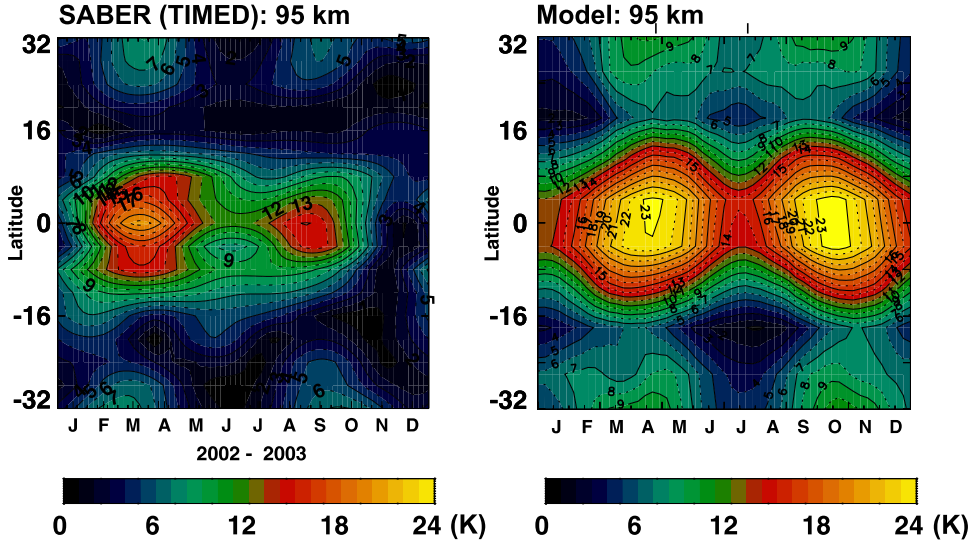

Figure 2. Seasonal variations of temperature amplitudes for migrating diurnal tide at 95 km, versus latitude. (left) SABER data for years 2002 and 2003. (right) The 4-year average of NSM.

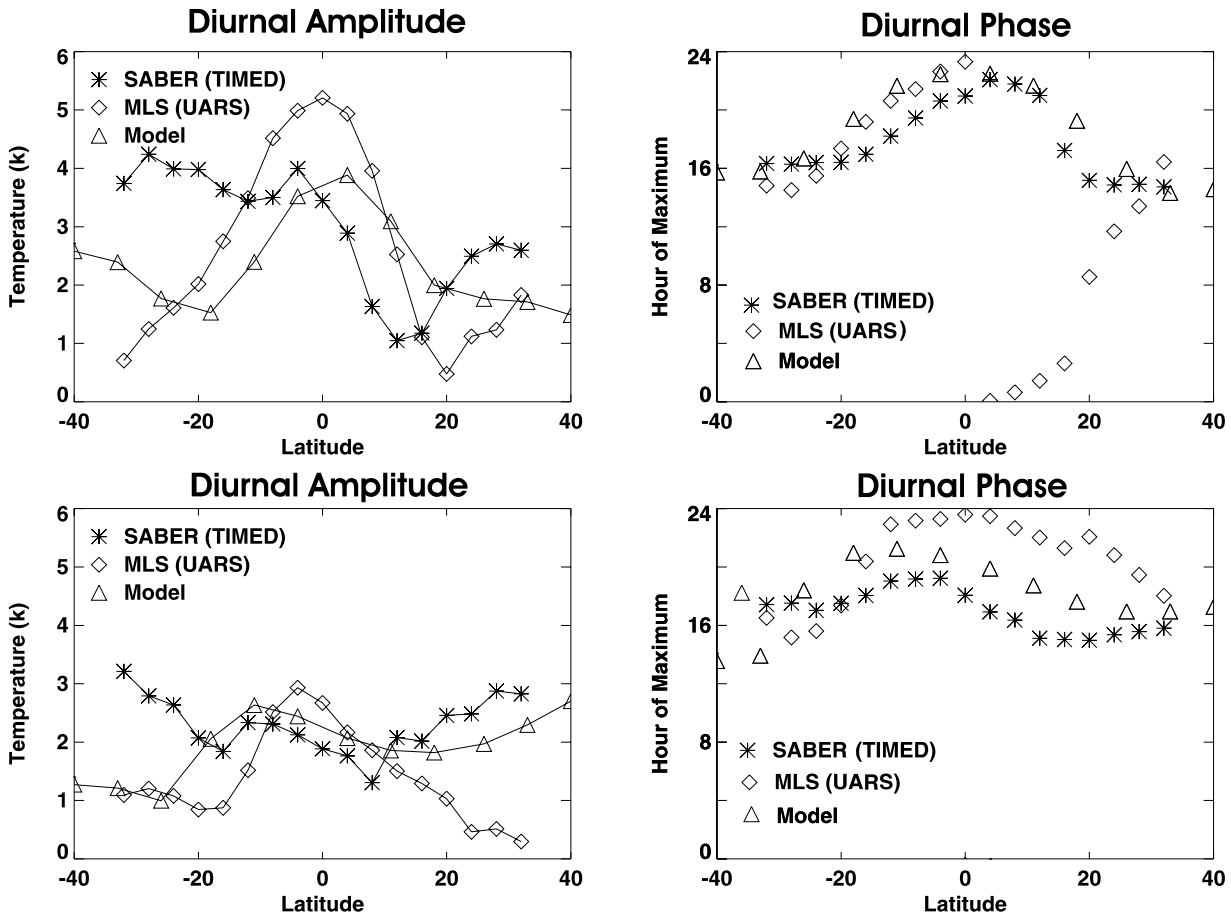

Figure 3. Analogous to Figure 1 but for 55 km. The results from SABER and NSM are also compared with the data from MLS (UARS) for years 1992, 1993, 1994.

amplitudes show an asymmetry with respect to the equator that is not as large in the MLS data or NSM results. The origin of this asymmetry is not known, but it disappears at altitudes above 60 km where the overall amplitudes from SABER continue to increase up to 85 km. The MLS instrument does not measure temperatures above about 60 km. The phase variations from the SABER data and the NSM compare reasonably well. The phase differences with the MLS data from 10°N to 30°N seen in Figure 4 appear to be an anomaly associated with MLS. Corresponding phases based on data from the Cryogenic Limb Array Etalon

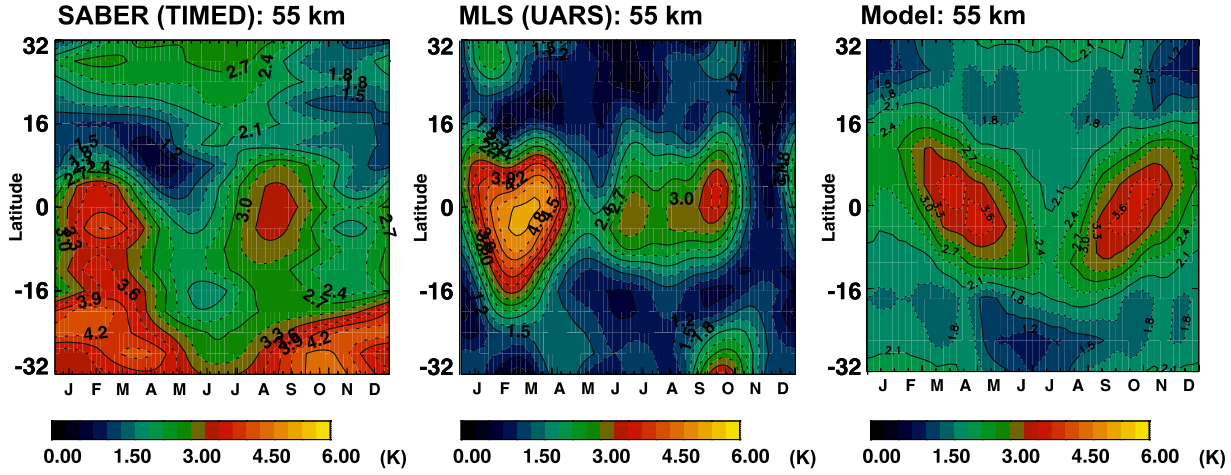

Figure 4. Analogous to Figure 2 but for 55 km, with the MLS data for years 1992, 1993, 1994 included in the middle panel.

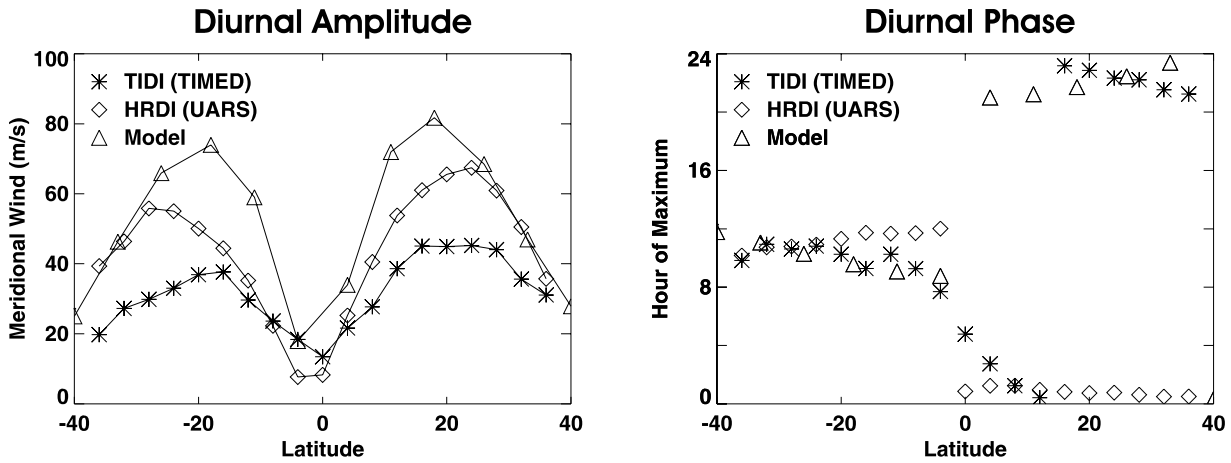

Figure 5. Amplitude and phase for the meridional winds of the migrating diurnal tide during spring equinox (day 80) at 95 km: TIDI for year 2003, HRDI (UARS) for years 1992, 1993, 1994, NSM (4-year average).

Spectrometer (CLAES) [*Roche et al.*, 1993], also on UARS, agree more with SABER and the NSM.

[22] Corresponding to Figure 2, we present in Figure 4 the seasonal variations of the tidal amplitude for 55 km, including the results from MLS. The left plot shows the SABER data from years 2002 and 2003 merged; the center plot is derived from MLS data for the years 1992 to 1994, and the right plot is from the NSM averaged over 4 years. Consistent with Figure 3, the large hemispherical asymmetry in the SABER temperature amplitudes is apparent for most of the year and is more apparent than the asymmetries based on MLS or the NSM results. As mentioned earlier, the asymmetry disappears at altitudes above 60 km, and it is not understood what causes it.

5.2. Winds

[23] Operationally, the data are sampled at predetermined and fixed latitudes, but the intervals between the latitudes are not regular. The instrument views the atmosphere from both sides of the observatory, thus increasing the sampling pattern. However, the measurements may not cover both the ascending and descending modes, thus reducing the sampling in local time at a given latitude. As noted earlier, the information content in terms of local solar time is more limited for TIDI compared to HRDI because it takes TIDI about 60 days to sample the full range of local times, compared to 36 days for HRDI. For these reasons, additional processing was needed, which included sorting and grouping of the data to effectively obtain ascending and descending sampling patterns near the selected latitudes. Even in cases where measurements are made for ascending and descending modes at nearly the same latitudes, the sampling window in local time may need to be increased to improve the potential for estimating the semidiurnal tide in addition to the diurnal component. In practice, we have grouped data from adjacent latitudes (up to 4°) to increase the local time sampling. The applied analysis does not involve averaging since each data point is incorporated individually into the algorithm. More details can be found in the work of *Huang and Reber* [2004, 2003] where a similar analysis was applied to UARS HRDI wind data.

5.2.1. Meridional Winds

[24] In Figure 5 we present for spring equinox the derived variations of the amplitude (m/s) and phase (hour of maximum value) for the diurnal tide meridional winds at 95 km plotted versus latitude. Shown are results based on data from TIDI (asterisks, year 2003), HRDI (diamonds, years 1992–1994) and the results from the NSM (triangles, 4-year average). Although the relative variations agree well, the TIDI amplitudes are systematically smaller. Although some of the differences could be attributed to the interannual variations, it should be noted that the uncertainties in the TIDI data can be significantly larger (sometimes approaching the data values) than those from HRDI. In addition, there appears to be a correlation between the data and the solar beta angle for the measurements.

[25] The seasonal variations of amplitude and phase for the measured meridional tidal winds are shown in Figure 6 at 20°N latitude and 95 km altitude. Plotted versus day of year are the results derived from TIDI (solid line) and HRDI (dotted line), and for comparison the HRDI results (asterisks) from *Burrage et al.* [1995] that are taken from Figure 2 of *Hagan et al.* [1999]. The results of Burrage et al. were derived from monthly averages of composite HRDI data from various years, which were represented by the (1,1) Hough function. As in the case for the latitudinal variations in Figure 5, the relative variations with day of year compare well for TIDI and HRDI, but again the TIDI amplitudes are systematically smaller. As is the case for temperatures, the differences between TIDI and HRDI amplitudes may be due to interannual variations. Interactions with the QBO could result in significant interannual variations [*McLandress*, 2002c; *Mayr and Mengel*, 2005]. In Figure 6, the characteristic semiannual variations are shown with maxima near equinox, which is consistent with the inferred seasonal variations of the temperature seen in Figure 2.

[26] Since TIDI needs 60 days to sample the full range of local times, compared to 36 days for HRDI, one might argue that the information content for TIDI is smaller, leading to smoother variations as shown in Figure 6. This is possible to an extent, but it is unlikely because the relative variations over a year agree well. Moreover, the information

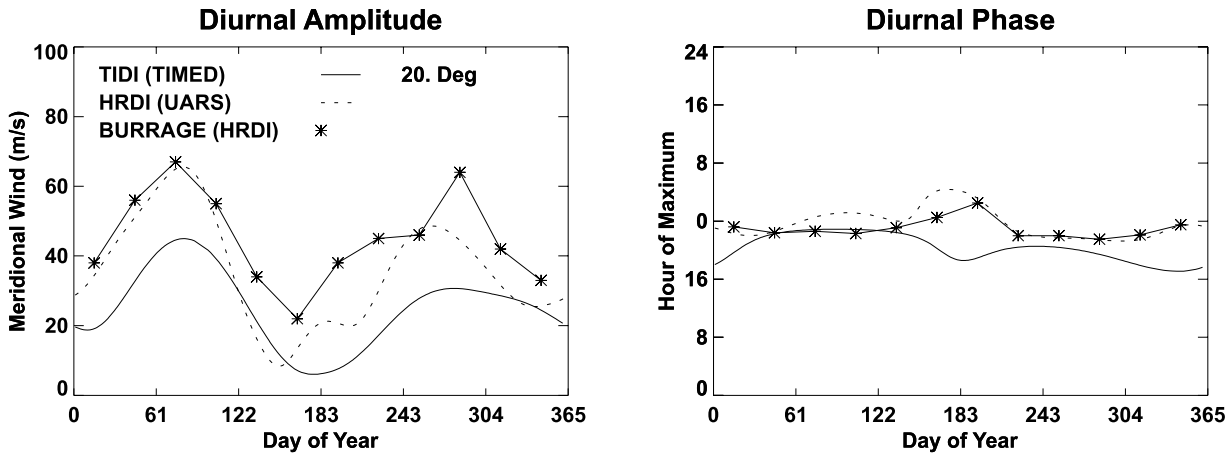

Figure 6. Derived diurnal amplitude (m/s) and phase (hour of maximum value) for meridional winds of migrating diurnal tide at 20°N latitude, 95 km, versus day of year: TIDI (solid line) and HRDI (dotted line). Asterisks describe HRDI results from *Burrage et al.* [1995], taken from Figure 2 of *Hagan et al.* [1999]. The results from Burrage et al. are monthly averages of composite HRDI data for various years represented by the (1,1) Hough function.

content in the SABER temperatures is adequate to resolve the seasonal variations, which can be as large or larger than those inferred from MLS on UARS.

[27] Analogous to Figure 2, we show in Figure 7 the derived seasonal variations for the meridional wind amplitude of the diurnal migrating tide at 95 km plotted versus latitude. The left plot is based on TIDI data (year 2003), the center plot represents HRDI data (1992–1994), and the right plot shows the results (4-year average) from the NSM.

[28] In terms of the variability of the diurnal tide, winds have been discussed extensively in the literature. As noted by *Forbes* [1984], there are average tidal structures with periods of a month or more, and they contain deviations from the average that have periods from a few days to a month. *Vial* [1989] noted that monthly averages are more appropriate in the climatological sense. Owing to the sampling limitations, we cannot extract the short-term variations from the TIMED and UARS observations. In our analysis, the shorter periods are smoothed out, and the resulting day versus year variations reflect that.

[29] *Wu et al.* [2006] have also derived from TIDI data the amplitude and phase variations for the meridional winds of the diurnal tide. They present the results over a range of altitudes but only for one 2-month interval. Therefore it is not feasible to compare with the seasonal variations in our results.

5.3. Zonal Winds

[30] Corresponding to Figure 6, we present in Figure 8 the amplitude (left plot) and phase (right plot) for the zonal winds of the diurnal tide at 20°N and 95 km altitude. The solid lines show results based on TIDI data and the dotted lines represent HRDI data. Unlike for the meridional winds, *Burrage et al.* [1995] did not obtain the zonal winds for the diurnal tide. The wind data presented in Figure 8 at 20°N compare reasonably well for amplitude and phase. How-

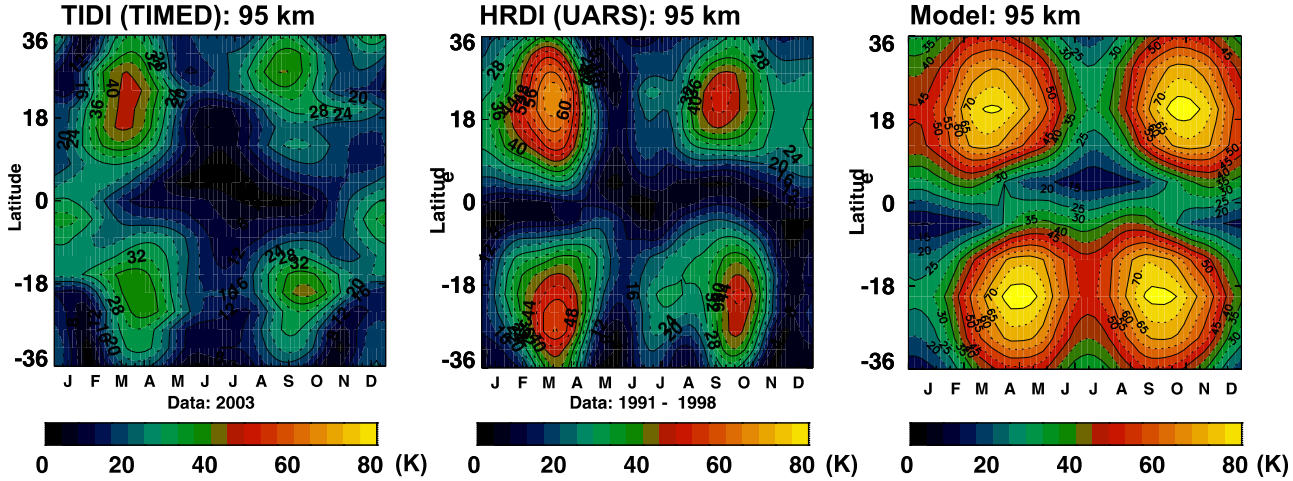

Figure 7. Derived seasonal variations of meridional wind amplitude for the migrating diurnal tide at 95 km versus latitude. (left) From TIDI data, year 2003; (center) From HRDI (UARS) data for years 1992, 1993, 1994; (right) For 4-year average of NSM.

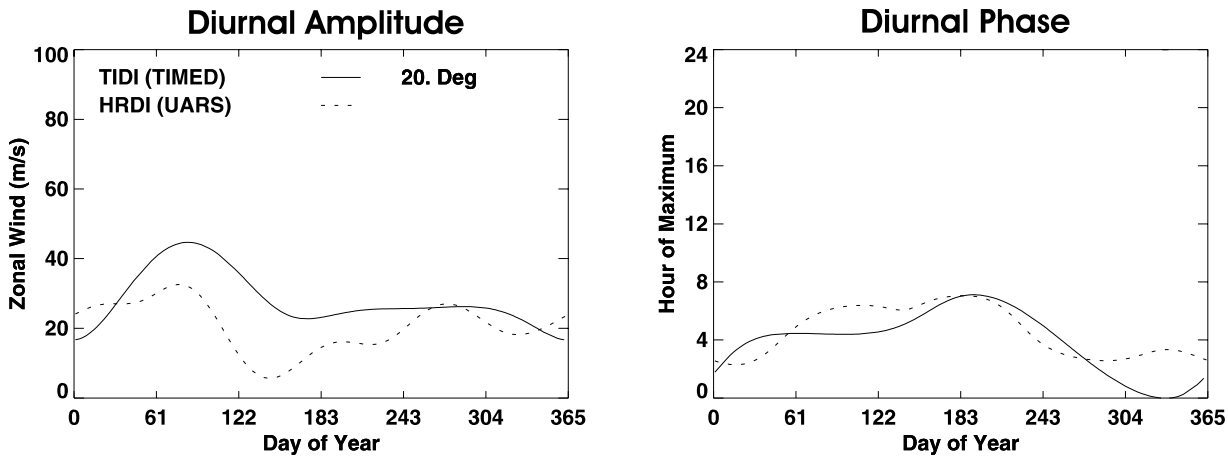

Figure 8. Derived diurnal amplitude (m/s) and phase of zonal wind migrating tide at 20°N latitude and 95 km versus day of year: TIDI (solid line) and HRDI (dotted line). (In the work of *Burrage et al.* [1995], zonal winds were not presented.)

ever, at most other latitudes (not shown), the agreement is not as good and thus requires additional analysis.

6. Discussion and Summary

[31] From measurements on the TIMED (SABER, TIDI) and UARS (MLS, HRDI) satellites, we have derived the signatures for the migrating diurnal tide in the observed variations of temperatures and winds. For TIMED and UARS, it takes 60 and 36 days, respectively, to sample the full range of local solar time, and we discussed some of the related difficulties and constraints that affect the information content. Under these constraints, we estimated the seasonal variations of the tide to compare the results from the two spacecraft, and with the NSM. The differences among the results from the TIMED and UARS measurements, not taken simultaneously, should be considered in view of the interannual variations that have been observed in the diurnal tide [*Burrage et al.*, 1995, 1996]. Modeling studies have shown [*McLandress*, 2002c; *Mayr and Mengel*, 2005] that such variations can be generated by the quasi-biennial oscillation of the zonal circulation at equatorial latitudes.

6.1. Temperatures

[32] The temperature results from SABER, MLS, and the NSM compare fairly well especially when one considers that the UARS and TIMED data were taken about 10 years apart. One area with obvious differences is seen at 55 km, where the SABER temperatures exhibit more pronounced asymmetries about the equator (Figures 3 and 4) that are not as apparent in the MLS data and in the NSM results. The reasons for this discrepancy are not known, but at about 60 km and above, the asymmetries in the SABER data are no longer apparent. The phase variations based on SABER data are more symmetric and agree well with the model (often better than the corresponding MLS results). Although not shown, the amplitudes generally increased with altitude between 55 and 95 km.

[33] As emphasized in section 3, the algorithm used in our analysis estimates the zonal mean component together with the tides. In a companion paper [*Huang et al.*, 2006], we show that there is also generally good agreement between the zonal mean temperature variations inferred from the SABER and MLS data.

6.2. Winds

[34] As shown in Figures 5, 6, and 7, the relative variations in the amplitude of the meridional winds for the diurnal tide derived from TIDI compare well with those from HRDI. The variations of the phase also are in general agreement. The TIDI wind amplitudes are systematically smaller, and interannual variations could account for that. For the zonal winds, our results shown in Figure 8 reveal good agreement between the TIDI and HRDI results. At most other latitudes, however, the zonal wind velocities from HRDI and TIDI differ significantly, and further analysis is needed to determine the cause. For the zonal mean component of the winds, derived in conjunction with the tides, we find the largest amplitudes for variations with a period of 4 months. For TIMED, this is also the period of the orbital precession (and solar beta angle). The solar beta angle (the complement of the angle between the normal to TIMED's orbital plane and the Earth-Sun line) is an important consideration in retrieving the wind velocities from radiance measurements. This correlation with the solar beta angle may well be due to the formation of ice on the instrument optics [*Skinner et al.*, 2003]. Therefore it would be prudent to revisit the data analysis for the wind measurements.

[35] The results presented here were generated for selected altitudes and years. SABER and TIDI measurements of temperatures and winds from the stratosphere into the thermosphere have now become available covering nearly 4 years. Comprehensive studies of the data over these altitude and time spans, combined with systematic modeling studies, will provide new insight about the processes that control the dynamics of the lower mesosphere, such as advection by zonal circulation and wave-mean flow interactions that can produce interannual variations [*McLandress*, 2002c; *Mayr and Mengel*, 2005].

[36] Our algorithm, presently applied to study the migrating tides, can also be applied to account for the longitudinal variations of the data to describe the nonmigrating tides, as we have done for HRDI winds [*Huang and Reber*, 2004]. Once the nonmigrating tides have been estimated, waves with longer periods such as planetary waves can then be estimated as well.

[37] **Acknowledgments.** We thank two anonymous reviewers for their insightful and helpful comments.

[38] Lou-Chuang Lee thanks the reviewers for their assistance in evaluating this paper.

References

Akmaev, R. A. (2001a), Simulation of large-scale dynamics in the mesosphere and lower thermosphere with the Doppler-spread parameterization of gravity waves: 1. Implementation and zonal mean climatologies, *J. Geophys. Res.*, *106*, 1193–1204.

Akmaev, R. A. (2001b), Simulation of large-scale dynamics in the mesosphere and lower thermosphere with the Doppler-spread parameterization of gravity waves: 2. Eddy Mixing and the diurnal tide, *J. Geophys. Res.*, *106*, 1205–1213.

Barath, F. T., et al. (1993), The Upper Atmosphere Research Satellite Microwave Limb Sounder, *J. Geophys. Res.*, *98*, 10,751–10,762.

Burrage, M. D., M. E. Hagan, W. R. Skinner, D. L. Wu, and P. B. Hays (1995), Long term variability in the solar diurnal tide observed by HRDI and simulated by the GSWM, *Geophys. Res. Lett.*, *22*, 2641–2644.

Burrage, M. D., R. A. Vincent, H. G. Mayr, W. R. Skinner, N. F. Arnold, and P. B. Hays (1996), Long term variability in the equatorial middle atmosphere zonal wind, *J. Geophys. Res.*, *101*, 12,847–12,854.

Chapman, S., and R. S. Lindzen (1970), *Atmospheric Tides*, Springer, New York.

Forbes, J. M. (1984), Middle atmosphere tides, *J. Atmos. Terr. Phys.*, *46*, 1049–1067.

Forbes, J. M., and H. B. Garrett (1979), Theoretical studies of atmospheric tides, *Rev. Geophys.*, *17*, 1951–1981.

Forbes, J. M., X. Zhang, E. R. Talaat, and W. Ward (2003), Nonmigrating diurnal tides in the thermosphere, *J. Geophys. Res.*, *108*(A1), 1033, doi:10.1029/2002JA009262.

Gaertner, V., M. Memmesheimer, and P. W. Blum (1983), A zonally averaged dynamical model for the middle atmosphere including gravity wave mean-flow interaction, Solstice condition, *Planet. Space Sci.*, *31*, 1465.

Garcia, R. R., and S. Solomon (1985), The effect of breaking gravity waves on the dynamics and chemical composition of the mesosphere and lower thermosphere, *J. Geophys. Res.*, *88*, 1379.

Geller, M. A. (1984), Modeling the middle atmosphere circulation, in *Dynamics of the Middle Atmosphere*, edited by J. R. Holton, and D. Matsuno, pp. 467–500, Terra Sci., Tokyo.

Geller, M. A., V. A. Yudin, B. V. Kattatov, and M. E. Hagan (1997), Modeling the diurnal tide with dissipation derived from UARS/HRDI measurements, *Ann. Geophys.*, *15*, 1198.

Hagan, M. E., M. D. Burrage, J. M. Forbes, J. Hackney, W. J. Randel, and X. Zhang (1999), GSWM-98: Results for migrating solar tides, *J. Geophys. Res.*, *104*, 6813–6827.

Hays, P. B., V. J. Abreu, M. E. Dobbs, D. A. Gell, H. J. Grassl, and W. B. Skinner (1993), The High Resolution Doppler Imager on the Upper Atmosphere Research Satellite, *J. Geophys. Res.*, *98*, 10,713–10,723.

Hines, C. O. (1997a), Doppler-spread parameterization of gravity-wave momentum deposition in the middle atmosphere, 1, Basic formulation, *J. Atmos. Sol. Terr. Phys.*, *59*, 371.

Hines, C. O. (1997b), Doppler-spread parameterization of gravity-wave momentum deposition in the middle atmosphere: 2. Broad and quasi monochromatic spectra, and implementation, *J. Atmos. Sol. Terr. Phys.*, *59*, 387.

Holton, J. R. (1982), The role of gravity wave induced drag and diffusion in the momentum budget of the mesosphere, *J. Atmos. Sci.*, *39*, 791.

Huang, F. T., and C. A. Reber (2001), "Synoptic" estimates of chemically active species and other diurnally varying parameters in the stratosphere, derived from measurements from the Upper Atmosphere Research Satellite (UARS), *J. Geophys. Res.*, *106*, 1655–1667.

Huang, F. T., and C. A. Reber (2003), Seasonal behavior of the semidiurnal and diurnal tides, and mean flows at 95 km, based on measurements from the High Resolution Doppler Imager (HRDI) on the Upper Atmosphere Research Satellite (UARS), *J. Geophys. Res.*, *108*(D12), 4360, doi:10.1029/2002JD003189.

Huang, F. T., and C. A. Reber (2004), Non-migrating semidiurnal and diurnal tides at 95 km based on wind measurements from the High Resolution Doppler Imager on UARS, *J. Geophys. Res.*, *109*, D10110, doi:10.1029/2003JD004442.

Huang, F. T., H. G. Mayr, C. A. Reber, J. Russell, M. Mylnczak, and J. Mengel (2006), Zonal-mean temperature variations inferred from SABER measurements on TIMED, compared with UARS observations, *J. Geophys. Res.*, *111*, A10S07, doi:10.1029/2005JA011427.

Killeen, T. L., et al. (1999), TIMED Doppler Interferometer (TIDI), *Proc. SPIE*, *3756*, 289–301.

Lindzen, R. S. (1981), Turbulence and stress owing to gravity wave and tidal breakdown, *J. Geophys. Res.*, *86*, 9707–9714.

Manson, A. H., Y. Luo, and C. Meek (2002), Global distributions of diurnal and semi-diurnal tides: Observations from HRDI-UARS of the MLS region, *Ann. Geophys.*, *20*, 1877–1890.

Manzini, E., N. A. McFarlane, and C. McLandress (1997), Impact of the Doppler spread parameterization in the simulation of the middle atmosphere circulation using the MA/ECHAM4 general circulation model, *J. Geophys. Res.*, *102*, 25,751.

Mayr, H. G., and J. G. Mengel (2005), Inter-annual variations of the diurnal tide in the mesosphere generated by the quasi-biennial oscillation, *J. Geophys. Res.*, *110*, D10111, doi:10.1029/2004JD005055.

Mayr, H. G., J. G. Mengel, K. L. Chan, and H. S. Porter (1998), Seasonal variations of the diurnal tide induced by gravity wave filtering, *Geophys. Res. Lett*, *25*, 943–946.

Mayr, H. G., J. G. Mengel, K. L. Chan, and H. S. Porter (2001), Mesosphere dynamics with gravity wave forcing: I, Diurnal and semi-diurnal tides, *J. Atmos. Sol. Terr. Phys.*, *63*, 1851.

Mayr, H. G., J. G. Mengel, E. R. Talaat, H. S. Porter, and K. L. Chan (2004), Modeling study of mesospheric planetary waves: Genesis and characteristics, *Ann. Geophys.*, *22*, 1885.

Mayr, H. G., J. G. Mengel, E. R. Talaat, H. S. Porter, and K. L. Chan (2005a), Mesospheric non-migrating tides generated with planetary waves: I. Characteristics, *J. Atmos. Solar-Terr. Phys.*, *67*, 959.

Mayr, H. G., J. G. Mengel, E. R. Talaat, H. S. Porter, and K. L. Chan (2005b), Mesospheric non-migrating tides generated with planetary waves: II. Influence of gravity waves, *J. Atmos. Sol. Terr. Phys.*, *67*, 981.

McLandress, C. (1997), Seasonal variability of the diurnal tide: Results from the Canadian middle atmosphere general circulation model, *J. Geophys. Res.*, *102*, 29,747–29,767.

McLandress, C. (1998), On the importance of gravity waves in the middle atmosphere and their parameterization in general circulation models, *J. Atmos. Sol. Terr.*, *60*, 1357–1383.

McLandress, C. (2002a), The seasonal variations of the propagating diurnal tide in the mesosphere and lower thermosphere. part I: The role of gravity waves and planetary waves, *J. Atmos. Sci.*, *69*, 893.

McLandress, C. (2002b), The seasonal variations of the propagating diurnal tide in the mesosphere and lower thermosphere. part II: The role of tidal heating and zonal mean winds, *J. Atmos. Sci.*, *69*, 907.

McLandress, C. (2002c), Interannual variations of the diurnal tide in the mesosphere induced by a zonal-mean wind oscillation in the tropics, *Geophys. Res. Lett.*, *29*(9), 1305, doi:10.1029/2001GL014551.

McLandress, C., G. G. Shepherd, and B. H. Solheim (1996), Satellite observations of the thermospheric tides: Results from the Wind Imaging Interferometer on UARS, *J. Geophys. Res.*, *101*, 4093–4114.

Meyer, C. K. (1999), Gravity wave interactions with the diurnal propagating tide, *J. Geophys. Res.*, *104*, 4223–4239.

Norton, W. A., and J. Thuburn (1999), Sensitivity of mesospheric mean flow, planetary waves, and tides to strength of gravity waves, *J. Geophys. Res.*, *104*, 30,897–30,911.

Reber, C. A. (1993), The Upper Atmosphere Research Satellite (UARS), *Geophys. Res. Lett.*, *20*(12), 1215–1218.

Roche, A. E., J. B. Kumer, J. L. Mergenthaler, G. A. Ely, W. G. Uplinger, J. F. Potter, T. C. James, and L. W. Sterritt (1993), The Cryogenic Limb Array Etalon Spectrometer (CLAES) on UARS: Experiment description and performance, *J. Geophys. Res.*, *98*, 10,763–10,775.

Russell, J. M., III, M. G. Mlynczak, L. L. Gordley, J. Tansock, and R. Esplin (1999), An overview of the SABER experiment and preliminary calibration results, *Proc. SPIE*, *3756*, 277–288.

Skinner, W. R., et al. (2003), Operation performance of the TIMED Doppler Interferometer (TIDI), in *SPIE Conference on Optical Spectroscopic Techniques and Instrumentation for Atmospheric and Space Research V*, vol. 5157, edited by A. M. Larar, J. A. Shaw, and Z. Sun, pp. 47–57, SPIE, San Diego, Calif.

Strobel, D. F. (1978), Parameterization of atmospheric heating rate from 15 to 120 km due to O2 and O3 absorption of solar radiation, *J. Geophys. Res.*, *83*, 6225.

Vial, F. (1989), Tides in the middle atmosphere, *J. Atmos. Terr. Phys.*, *51*, 3–17.

Wu, Q., T. L. Killeen, D. A. Ortland, S. C. Solomon, R. D. Gablehouse, R. M. Johnson, W. R. Skinner, R. J. Niciejewski, and S. J. Franke (2006),

TIMED Doppler Interferometer (TIDI) observations of migrating diurnal and semi-diurnal tides, *J. Atmos. Sol. Terr. Phys.*, *68*, 408–417.

Yudin, V. A. (1997), et al., Thermal tides and studies to tune the mechanistic tidal model using UARS observations, *Ann. Geophys.*, *15*, 1205.

Zhu, X. (1989), Radiative cooling calculated by random band models with S-1-beta tailed distribution, *J. Atmos., Sci.*, *46*, 511.

F. T. Huang, Creative Computing Solutions Inc., Rockville, MD 20850, USA. (fthuang@comcast.net)

T. Killeen, High Altitude Observatory, National Center for Atmospheric Research, Boulder, CO 80307, USA.

H. G. Mayr and C. A. Reber, NASA Goddard Space Flight Center, Greenbelt, MD 20771, USA.

J. Mengel, Science Systems and Applications, Lanham, MD 20706, USA.

M. Mlynczak, NASA Langley Research Center, Hampton, VA 23681. USA.

J. Russell, Center for Atmospheric Sciences, Hampton University, Hampton, VA 23668, USA.

W. Skinner, Department of Atmospheric, Oceanic, and Space Sciences, University of Michigan, Ann Arbor, MI 48109, USA.